

Gen2Act: Human Video Generation in Novel Scenarios enables Generalizable Robot Manipulation

Anonymous Author(s)

Affiliation

Address

email

1 **Abstract:** How can robot manipulation policies generalize to novel tasks involv-
2 ing unseen object types and new motions? In this paper, we provide a solution
3 in terms of predicting motion information from web data through human video
4 generation and conditioning a robot policy on the generated video. Instead of at-
5 tempting to scale robot data collection which is expensive, we show how we can
6 leverage video generation models trained on easily available web data, for en-
7 abling generalization. *Our approach Gen2Act casts language-conditioned manip-
8 ulation as zero-shot human video generation followed by execution with a single
9 policy conditioned on the generated video.* To train the policy, we use an order
10 of magnitude less robot interaction data compared to what the video prediction
11 model was trained on. *Gen2Act* doesn't require fine-tuning the video model at all
12 and we directly use a pre-trained model for generating human videos. Our results
13 on diverse real-world scenarios show how *Gen2Act* enables manipulating unseen
14 object types and performing novel motions for tasks not present in the robot data.

15 **Keywords:** video generation, diverse manipulation

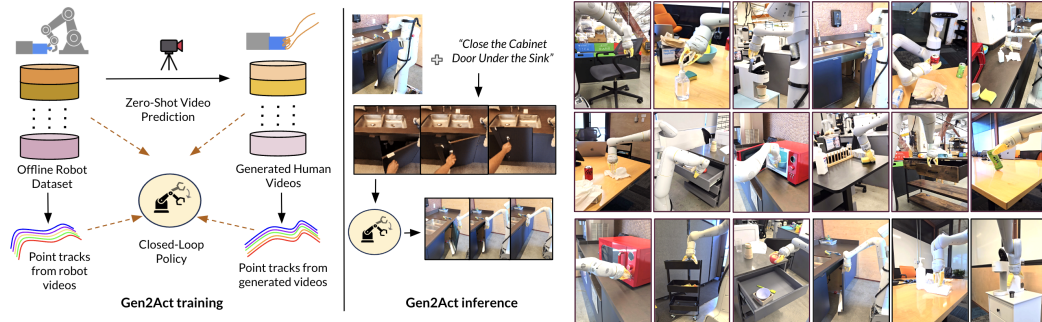


Figure 1: *Gen2Act* learns to generate a human video followed by robot policy execution conditioned on the generated video. This enables diverse real-world manipulation in unseen scenarios.

16 1 INTRODUCTION

17 To realize the vision of robot manipulators helping us in the humdrum everyday activities of messy
18 living rooms, offices, and kitchens, it is crucial to develop robot policies capable of generalizing
19 to novel tasks in unseen scenarios. In order to be practically useful, it is desirable to not require
20 adapting the policy to new tasks through test-time optimizations and instead being able to directly
21 execute it given a colloquial task specification such as language instructions. Further, such a policy
22 should be able to tackle a broad array of everyday tasks like manipulating articulated objects, pour-
23 ing, re-orienting objects, wiping tables without the need to collect robot interaction data for every

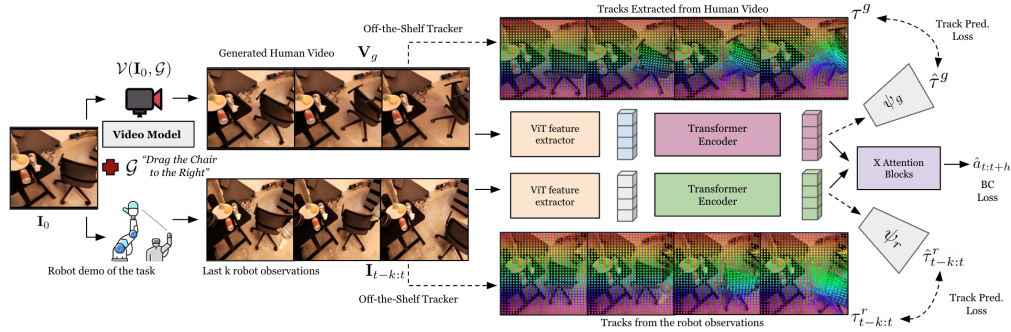


Figure 2: Architecture of the translation model of *Gen2Act* (closed-loop policy π_θ). Given an image of a scene \mathbf{I}_0 and a language-goal description of the task \mathcal{G} , we generate a human video \mathbf{V}_g with a pre-trained video generation model $\mathcal{V}(\mathbf{I}_0, \mathcal{G})$. During training of the policy, we incorporate track prediction from the policy latents as an auxiliary loss in addition to a behavior cloning loss. Dotted pathways show training-specific computations. During inference, we do not require track prediction and only use the video model \mathcal{V} in conjunction with the policy $\pi_\theta(\mathbf{I}_{t-k:t}, \mathbf{V}_g)$.

24 task unlike recent efforts on behavior cloning with robot datasets [1, 2, 3, 4]. This is because col-
 25 lecting large robot datasets that cover the diversity of everyday scenarios is extremely challenging
 26 and might be deemed impractical.

27 In order to mitigate issues with purely scaling robotic datasets, a line of recent works have sought
 28 to incorporate additional behavioral priors in representation learning by pre-training visual encoders
 29 with non-robotic datasets [5, 6, 7, 8, 9] and co-training policies with vision-language models [10,
 30 11, 12]. Going beyond abstract representations, other works have learned attributes from web videos
 31 more directly informative of motion in the form of predicting goal images [13, 14, 15], hand-object
 32 mask plans [16], and embodiment-agnostic point tracks [17]. These approaches show promising
 33 signs of generalization to tasks unseen in the robot interaction datasets, but training such specific
 34 predictive models from web video data requires utilizing other intermediate models for providing
 35 ground-truths and thus are hard to scale up.

36 Our key insight for enabling generalization in manipulation is to cast motion prediction from web
 37 data in the very generic form of zero-shot video prediction. This lets us directly leverage advances
 38 in video generation models, by conditioning a robot policy on the generated video for new tasks
 39 that are unseen in the robot datasets. We posit that as video generation models get better due to
 40 large interest in generative AI [18, 19, 20] beyond robotics, an approach that relies on learning a
 41 policy conditioned on zero-shot video prediction can effectively scale and generalize to increasingly
 42 diverse real-world scenarios. For performing a manipulation task in a novel scene, a generated video
 43 conditioned on the language description of the task is particularly useful for conveying *what* needs
 44 to be done and in capturing motion-centric information of *how* to perform the task that can then
 45 be converted to robot actions through a learned policy. Compared to a generated video, a language
 46 description or a goal image alone only conveys what the task is.

47 We develop *Gen2Act* by instantiating language-conditioned manipulation as human video gener-
 48 ation followed by generated human video to robot translation with a closed-loop policy (Fig. 1).
 49 We opt for generating human videos as opposed to directly generating robot videos since video
 50 generation models are often trained with human data on the web, and they are able to generate hu-
 51 man videos zero-shot given a new scene. We then train a translation model that needs some offline
 52 robot demonstrations and corresponding generated human videos. We generate these corresponding
 53 human videos offline with an off-the-shelf model [20] by conditioning on the first frame of each
 54 trajectory (the first frame doesn't have the robot in the scene) and the language description of the
 55 task. We instantiate this translation model as a closed loop policy that is conditioned on the history
 56 of robot observations in addition to the generated human video so that it can take advantage of the
 57 visual cues in the scene and adjust its behavior reactively.

58 In order to capture motion information beyond that implicitly provided by visual features from the
 59 generated video, we extract point tracks from the generated human video and the video of robot

60 observations (through an off-the-shelf tracker [21]) and optimize a track prediction auxiliary loss
61 during training. The aim of this loss function is to ensure that the latent tokens of the closed-loop
62 policy are informative of the motion of points in the scene. We train the policy to optimize the
63 typical behavior cloning loss for action prediction combined with this track prediction loss. For
64 deployment, give a language description of a task to be performed, we generate a human video and
65 run the policy conditioned on this video.

66 The diverse real-world manipulation results of *Gen2Act* (featured in Fig. 1) demonstrate the broad
67 generalization capabilities enabled by learning to infer motion cues from web video data through
68 zero-shot video generation combined with motion extraction through point track prediction for solv-
69 ing novel manipulation tasks in unseen scenarios. For generalization to novel object types and
70 novel motion types unseen in the robot interaction training data, we show that *Gen2Act* achieves
71 on average $\sim 30\%$ higher absolute success rate over the most competitive baseline. Further, we
72 demonstrate how *Gen2Act* can be chained in sequence for performing long-horizon activities like
73 “making coffee” consisting of several intermediate tasks.

74 2 Related Works

75 We discuss prior works in imitation learning with visual observations, learning representations from
76 non-robotic datasets, and approaches for conditional behavior cloning.

77 **Visual Imitation.** Visual imitation is a scalable approach for robotic manipulation [22, 23, 24] and
78 end-to-end policy learning more broadly [25, 26]. While early works in multi-task imitation learning
79 collected limited real-world data [27, 28], more recent approaches [29, 1, 30] collect much larger
80 datasets. In fact, recent works that have attempted to directly scale this for training large models
81 have required years of expensive data collection [1, 10, 2] and have still been restricted to limited
82 generalization especially with respect to novel object types and novel motions in unseen scenarios.

83 **Visual Representations for Manipulation.** To enable generalization, many recent works propose
84 using pre-trained visual representations trained primarily on non-robot datasets [31, 32], for learning
85 manipulation policies [5, 8, 6, 33, 6, 34, 7, 9, 35, 36]. However, they are primarily limited to learning
86 task-specific policies [5, 8, 37, 38] as they rely on access to a lot of in-domain robot interaction data.
87 Apart from training visual encoders, a line of works augment existing robot datasets with semantic
88 variations using generative models [39, 40, 41, 2, 42]. While this enables policies to generalize to
89 unseen scenes and become robust to distractors, generalization to unseen object types and motion
90 types still remains a challenge.

91 **Conditional Behavior Cloning.** Some prior works train robotic policies conditioned on human
92 videos but require paired in-domain human-robot data [43, 44, 45, 46, 47, 48] and are not capable
93 of leveraging web data. Others use curated data of human videos to leverage human hand motion
94 information [49, 50] for learning task-specific policies (instead of a single model across generic
95 tasks). Towards learning structure more directly related to manipulation from web videos, some
96 works try to predict visual affordances in the form of where to interact in an image, and local
97 information of how to interact [51, 52, 53, 54, 55]. While these could serve as good initializations
98 for a robotic policy, they are not sufficient on their own for accomplishing tasks, and so are typically
99 used in conjunction with online learning, requiring several hours of deployment-time training and
100 robot data [56, 53, 13]. Others learn to predict motion from web data more directly in the form of
101 masks of hand and objects in the scene [16] and tracks of how arbitrary points in the scene should
102 move [17], for conditional behavior cloning. However, training such predictive models from web
103 videos requires reliance on intermediate models for providing ground-truth information and are thus
104 hard to scale up broadly.

105 3 APPROACH

106 We develop a language-conditioned robot manipulation system, *Gen2Act* that generalizes to novel
107 tasks in unseen scenarios. To achieve this, we adopt a factorized approach: 1) Given a scene and a

108 task description, using an existing video prediction model generate a video of a human solving the
 109 task, 2) Conditioned on the generated human video infer robot actions through a learned human-
 110 to-robot translation model that can take advantage of the motion cues in the generated video. We
 111 show that this factorized strategy is scalable in leveraging web-scale motion understanding inherent
 112 in large video models, for synthesizing *how* the manipulation should happen for a novel task, and
 113 utilizing orders of magnitude less robot interaction data for the much simpler task of translation
 114 from a generated human video to *what* actions the robot should execute.

115 3.1 Overview and Setup

116 Given a scene specified by an image \mathbf{I}_0 and a goal \mathcal{G} describing in text the task to be performed,
 117 we want a robot manipulation system to execute actions $\mathbf{a}_{1:H}$ for solving the task. To achieve
 118 this in unseen scenarios, we learn motion predictive information from web video data in the form
 119 of a video prediction model $\mathcal{V}(\mathbf{I}_0, \mathcal{G})$ that zero-shot generates a human video of the task, \mathbf{V}_g . In
 120 order to translate this generated video to robot actions, we train a closed-loop policy $\pi_\theta(\mathbf{I}_{t-k:t}, \mathbf{V}_g)$
 121 conditioned on the video and the last k robot observations, through behavior cloning on a small
 122 robot interaction dataset \mathcal{D}_r . In order to implicitly encode motion information from \mathbf{V}_g in the
 123 policy π_θ , we extract point tracks from both \mathbf{V}_g and $\mathbf{I}_{t-k:t}$, respectively τ_g and τ_r , and incorporate
 124 track prediction as an auxiliary loss \mathcal{L}_τ during training. Fig. 2 shows an overview of this setup.

125 3.2 Human Video Generation

126 We use an existing video generation model for
 127 the task of text+image conditioned video gen-
 128 eration. We find that current video generation
 129 models are good at generating human videos
 130 zero-shot without requiring any fine-tuning or
 131 adaptation (some examples in Fig. 3). Instead
 132 of trying to generate robot videos as done by
 133 some prior works [57, 58], we focus on just
 134 human video generation because current video
 135 generation models cannot generate robot videos
 136 zero-shot and require robot-specific fine-tuning
 137 data for achieving this. Such fine-tuning often
 138 subtracts the benefits of generalization to novel
 139 scenes that is inherent in video generation mod-
 140 els trained on web-scale data.

141 For training, given an offline dataset of robot
 142 trajectories \mathcal{D}_r along with language task in-
 143 structions \mathcal{G} , we create a corresponding gen-
 144 erated human video dataset \mathcal{D}_g by generating
 145 videos conditioned on the first frame of the
 146 robot trajectories and the language instruction. This procedure of generating paired datasets
 147 $\{\mathcal{D}_r, \mathcal{D}_g\}$ is fully automatic and does not require manually collecting human videos as done by
 148 prior works [59, 46]. We do not require the generated human videos to have any particular structure
 149 apart from looking visually realistic, manipulating the relevant objects plausibly, and having mini-
 150 mal camera motion. As seen in the qualitative results in Fig. 3, all of this is achieved zero-shot with
 151 a pre-trained video model.

152 During evaluation, we move the robot to a new scene \mathbf{I}_0 , specify a task to be performed in language
 153 \mathcal{G} , and then generate a human video $\mathbf{V}_g = \mathcal{V}(\mathbf{I}_0, \mathcal{G})$ that is fed into the human-to-robot translation
 154 policy, described in Section 3.3. Our approach is not tied to a specific video generative model and
 155 as video models become better, this stage of our approach will likely scale upwards. We expect the
 156 overall approach to generalize as well since the translation model is tasked with a simpler job of

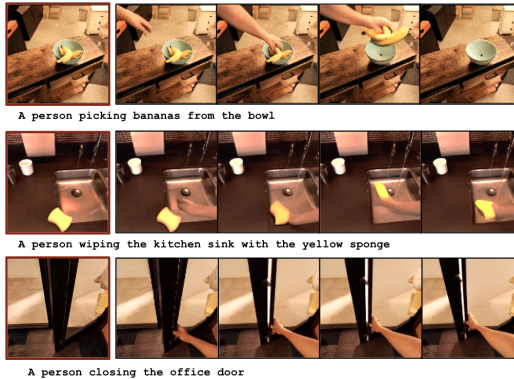


Figure 3: Visualization of zero-shot video generation for different tasks. The blue frame and the language description are input to the video generation model of *Gen2Act* and the black frames show sub-sampled frames of the generated video. These results demonstrate the applicability of off-the-shelf video generation models for image+text conditioned video generation that preserves the scene and performs the desired manipulation task.

157 inferring motion cues from the generated human video in novel scenarios, and implicitly converting
 158 that to robot actions. As we show through results in [Section 3.3](#) only a small amount of diverse robot
 159 trajectories (~ 400) combined with existing offline datasets is enough to train a robust translation
 160 model.

161 3.3 Generated Human Video to Robot Action Translation

162 We instantiate generated human video to robot action translation as a closed loop policy π_θ . Given
 163 a new scene and a task description, the generated human video provides motion cues for how the
 164 manipulation should happen in the scene, and the role of the policy is to leverage relevant informa-
 165 tion from the generated video, combined with observations in the robot’s frame, for interacting in
 166 the scene. Instead of attempting to explicitly extract waypoints from the generated video based on
 167 heuristics, we adopt a more end-to-end approach that relies on general visual features of the video,
 168 and general point tracks extracted from the video. This implicit conditioning on the generated video
 169 is helpful in mitigating potential artifacts in the generation and in making the approach more robust
 170 to mismatch in the video and the robot’s embodiment. Note that we perform human video generation
 171 and ground-truth track extraction completely offline for training.

172 **Visual Feature Extraction.** For each frame in the generated human video \mathbf{V}_g and the robot video
 173 $\mathbf{I}_{t-k:k}$, we first extract features, i_g and i_r through a ViT encoder χ . The number of video tokens ex-
 174 tracted this way is very large and they are temporally uncorrelated, so we have Transformer encoders
 175 Φ_g and Φ_r that process the respective video tokens through gated Cross-Attention Layers based on
 176 a Perceiver-Resampler architecture [60] and output a fixed number $N = 64$ of tokens. These tokens
 177 respectively are $z_g = \Phi_g(i_g)$ and $z_r = \Phi_r(i_r)$.

178 In addition to visual features from the generated video, we encode explicit motion information in
 179 the human-to-robot translation policy through point track prediction.

180 **Point Track Prediction.** We run an off-the-shelf tracking model [61, 21] on the generated video
 181 \mathbf{V}_g to obtain tracks τ_g of a random set of points in the first frame P^0 . In order to ensure that the
 182 latent embeddings from the generated video z_g can distill motion information in the video, we set
 183 up a track prediction task conditioned on the video tokens. For this, we define a track prediction
 184 transformer $\psi_g(P^0, i_g^0, z_g)$ to predict tracks $\hat{\tau}_g$ and define an auxiliary loss $\|\tau_g - \hat{\tau}_g\|_2$ to update
 185 tokens g_e .

186 Similarly, for the current robot video $\mathbf{I}_r^{t-k:k}$, we set up a similar track prediction auxiliary loss. We
 187 run the ground-truth track prediction once over the entire robot observation sequence (again with
 188 random points in the first frame P_0), but during training, the policy is input a chunk of length k
 189 in one pass. So here, the track prediction transformer $\psi_r(P^{t-k}, i_r^{t-k}, z_r^{t-k:t})$ is conditioned on
 190 the points in the beginning of the chunk P_{t-k} , the image features at that time-step i^{t-k} and the
 191 observation tokens for the chunk z_r .

192 **BC Loss.** For ease of prediction, we discretize the action space such that each dimension has 256
 193 bins. We optimize a Behavior Cloning (BC) objective by minimizing error between the predicted
 194 actions $\hat{a}_{t:t+h}$ and the ground-truth $a_{t:t+h}$ through a cross-entropy loss.

195 In *Gen2Act*, we incorporate track prediction as an auxiliary loss during training combined with the
 196 BC loss and the track prediction transformer is not used at test-time. This is helpful in reducing
 197 test-time computations for efficient deployment.

198 3.4 Deployment

199 For deploying *Gen2Act* to solve a manipulation task, we first generate a human video conditioned on
 200 the language description of the task and the image of the scene. We then roll out the generated video
 201 conditioned closed-loop policy. For chaining *Gen2Act* to perform long-horizon activities consisting
 202 of several tasks, we first use an off-the-shelf LLM (e.g. Gemini) to obtain language descriptions of
 203 the different tasks. We chain *Gen2Act* for the task sequence by using the last image of the previous
 204 policy rollout as the first frame for generating a human video of the subsequent task. We do this

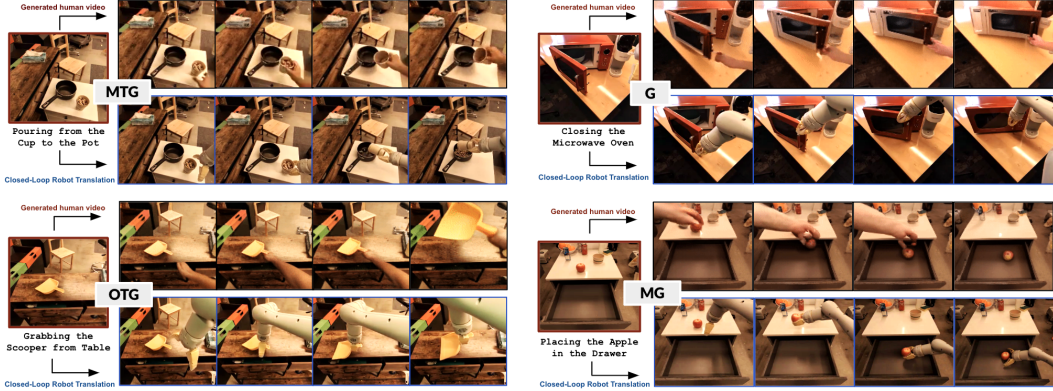


Figure 4: Visualization of the closed-loop policy rollouts (bottom row) conditioned on the generated human videos (top row) for four tasks. The red frame and the language description are input to the video generation model of *Gen2Act*. The black frames show sub-sampled frames of the generated video, and the blue frames show robot executions conditioned on the generated video.

205 chaining in sequence as opposed to generating all the videos from the first image because the final
 206 state of the objects in the scene might be different after the robot execution of an intermediate task.

207 4 EXPERIMENTS

208 We perform experiments in diverse kitchen, office, and lab scenes, across a wide array of manipula-
 209 tion tasks. Through these experiments we aim to answer the following questions:

- 210 • Is *Gen2Act* able to generate plausible human videos of manipulation in diverse everyday
 211 scenes?
- 212 • How does *Gen2Act* perform in terms of varying levels of generalization with new scenes,
 213 objects, and motions?
- 214 • Can *Gen2Act* enable long-horizon manipulation through chaining of the video generation
 215 and video-conditioned policy execution?
- 216 • Can the performance of *Gen2Act* for new tasks be improved by co-training with a small
 217 amount of additional diverse human tele-operated demonstrations?

218 4.1 Details of the Evaluation Setup

219 Following prior works in language/goal-conditioned policy learning, we quantify success in terms of
 220 whether the executed robot trajectory solves the task specified in the instruction, and define success
 221 rate over different rollouts for the same task description. We categorize evaluations with respect to
 222 different levels of generalization by following the terminology of prior works [17, 1]: Mild Genera-
 223 lization (**MG**): unseen configurations of seen object instances in seen scenes; organic scene varia-
 224 tions like lighting and background changes. Standard Generalization (**G**): unseen object instances in
 225 seen/unseen scenes. Object-Type Generalization (**OTG**): completely unseen object types, in unseen
 226 scenes. Motion-Type Generalization (**MTG**): completely unseen motion types, in unseen scenes

227 Here, seen vs. unseen is defined with respect to the robot interaction data, and the assumption is that
 228 the video generation model has seen diverse web data including things that are unseen in the robot
 229 data.

230 4.2 Dataset and hardware details

231 For video generation, we use an existing video model, VideoPoet [20] For obtaining tracks on the
 232 generated human video and the robot demo, we use an off-the-shelf tracking approach [61, 21]. For
 233 robot experiments, we use a mobile manipulator with compliant two finger-grippers, and operate

Table 1: Comparison of success rates for *Gen2Act* with different baselines and an ablated variant for the different levels of generalization as defined in Section 4.1

	Mild (MG)	Standard (G)	Obj. Type (OTG)	Motion. Type (MTG)	Avg.
RT1	68	18	0	0	22
RT1-GC	75	24	5	0	26
Vid2Robot	83	38	25	0	37
Gen2Act (w/o track)	83	58	50	5	49
Gen2Act	83	67	58	30	60

234 this robot for policy deployment through end-effector control. The arm is attached to the body of the
 235 robot on the right. We manually move the robot around across offices, kitchens, and labs and ask it
 236 to manipulate different objects in these scenes. We operate the robot for manipulation at a frequency
 237 of 3Hz. Before each task, we reset the robot arm to a fixed pre-defined reset position such that the
 238 scene is not occluded through the robot’s camera.

239 **4.3 Baselines and Comparisons**

240 We perform comparisons with baselines and ablations with variants of *Gen2Act*. In particular, we
 241 compare with a language-conditioned policy baseline (*RT1*) [1] trained on the same robot data as
 242 *Gen2Act*. We also compare with a video-conditioned policy baseline trained on paired real hu-
 243 man and robot videos (*Vid2Robot*) [46], a goal-image conditioned policy baseline trained with the
 244 same real and generated videos of *Gen2Act* but by conditioning on just the last video frames (i.e.
 245 goal image) of the generated human videos (*RT1-GC*). Finally, we consider an ablated variant of
 246 *Gen2Act* without the track prediction loss.

247 **4.4 Analysis of Human Video Generations**

248 Fig. 3 shows qualitative results for human video generation in diverse scenarios. We can see that the
 249 generated videos correspond to plausibly manipulating the scene in the initial image as described
 250 by the text instruction. We can see that the respective object in the scene is manipulated while pre-
 251 serving the background and without introducing camera movements and artifacts in the generations.
 252 This is exciting because these generations are zero-shot in novel scenarios and can be directly used
 253 in a robot’s context to imagine how an unseen object in an unseen scene should be manipulated by
 254 a human.

255 **4.5 Generalization of *Gen2Act* to scenes, objects, motions**

256 In this section we compare performance of *Gen2Act* with baselines and ablated variants for different
 257 levels of generalization. Table 1 shows success rates for tasks averaged across different levels of
 258 generalization. We observe that for higher levels of generalization, *Gen2Act* achieves much higher
 259 success rates indicating that human video generation combined with explicitly extracting motion
 260 information from track prediction is helpful in unseen tasks.

261 **4.6 Chaining *Gen2Act* for long-horizon manipulation**

262 We now analyze the feasibility of *Gen2Act* for solving a sequence of manipulation tasks through
 263 chaining. Table 3 shows results for long-horizon activities like “Making Coffee” that consist of
 264 multiple tasks to be performed in sequence. We obtain this sequence of tasks through Gemini [62],
 265 and for each task, condition the video generation on the last image of the scene from the previous
 266 execution and execute the policy for the current task conditioned on the generated human video. We
 267 repeat this in sequence for all the stages, and report success rates for successful completion upto
 268 each stage over 5 trials. Fig. 5 visually illustrates single-take rollouts from four such long-horizon
 269 activities.

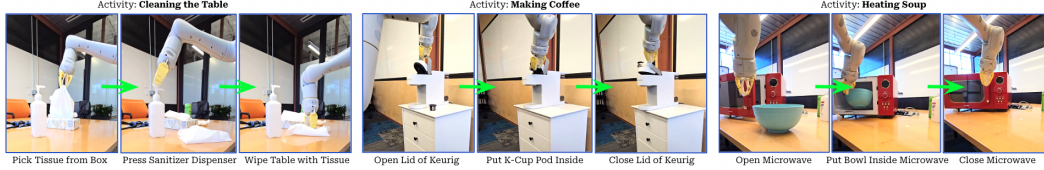


Figure 5: Robot executions for a sequence of tasks. The last frame of the previous execution serves as the conditioning frame for next stage video generation.

Table 2: Analysis of co-training with an additional dataset of diverse tele-operated robot demonstrations (~400 trajectories).

Co-Training	Mild (MG)	Standard (G)	Obj. Type (OTG)	Motion. Type (MTG)	Avg.
Gen2Act (w/o co-train)	83	67	58	30	60
Gen2Act (w/ co-train)	85	75	62	35	64

270 4.7 Co-Training with additional teleop demonstrations

271 The offline dataset we used for experiments in the previous section had limited coverage over scenes
 272 and types of tasks thereby allowing less than 60% success rate of *Gen2Act* for higher levels of gen-
 273 eralization (OTG and MTG in Table 1). In this section, we perform experiments to understand if
 274 adding a small amount of additional *diverse* tele-operated trajectories, for co-training with the exist-
 275 ing offline dataset, can help improve generalization. We keep the video generation model fixed as
 276 usual. From the results in Table 2 we see improved performance of *Gen2Act* with such co-training.
 277 This is exciting because it suggests that with only a small amount of diverse demonstrations, the
 278 translation model of *Gen2Act* can be improved to better condition on the generated videos for higher
 279 levels of generalization where robot data support is limited.

280 4.8 Analysis of Failures

281 Here we discuss the type of failures exhibited by *Gen2Act*. We observe that for MG and to some
 282 extent in G, inaccuracies in video generation are less correlated with failures of the policy. While, for
 283 the higher levels of generalization, object type (OTG) and motion type (MTG), if video generation
 284 yields implausible videos, then the policy doesn't succeed in performing the tasks. This is also
 285 evidence that the policy of *Gen2Act* is using the generated human video for inferring motion cues
 286 while completing a task, and as such when video generation is incorrect in scenarios where robot
 287 data support is limited (e.g. in OTG and MTG), the policy fails.

288 5 Discussion and Conclusion

289 **Summary.** In this work, we developed a framework for learning generalizable robot manipulation
 290 by combining zero-shot human video generation from web data with limited robot demonstrations.
 291 Broadly, our work is indicative of how motion predictive models trained on non-robotic datasets
 292 like web videos can be used to enable generalization of manipulation policies to unseen
 293 scenarios, without requiring collection of robot data for every task.

294 **Limitations.** Our work focused on zero-shot human video generation combined with point track
 295 prediction on the videos as a way for providing motion cues to a robot manipulation system for
 296 interacting with unseen objects and performing novel tasks. As such, the capabilities of our system
 297 are limited by the current capabilities of video generation models, like inability to generate realistic
 298 hands and thereby limited ability to perform very dexterous tasks.

299 **Future Work.** It would be an interesting direction of future work to explore recovering more dense
 300 motion information from the generated videos beyond point tracks, like object meshes for address-
 301 ing some of the limitations. Another important direction would be to enable reliable long-horizon
 302 manipulation by augmenting chaining with learning recovery policies for intermediate failures.

References

- [1] A. Brohan, N. Brown, J. Carbajal, Y. Chebotar, J. Dabis, C. Finn, K. Gopalakrishnan, K. Hausman, A. Herzog, J. Hsu, et al. Rt-1: Robotics transformer for real-world control at scale. *arXiv preprint arXiv:2212.06817*, 2022.
- [2] H. Bharadhwaj, J. Vakil, M. Sharma, A. Gupta, S. Tulsiani, and V. Kumar. Roboagent: Generalization and efficiency in robot manipulation via semantic augmentations and action chunking. In *2024 IEEE International Conference on Robotics and Automation (ICRA)*, 2024.
- [3] E. Jang, A. Irpan, M. Khansari, D. Kappler, F. Ebert, C. Lynch, S. Levine, and C. Finn. Bc-z: Zero-shot task generalization with robotic imitation learning. In *Conference on Robot Learning*, pages 991–1002. PMLR, 2022.
- [4] A. Khazatsky, K. Pertsch, S. Nair, A. Balakrishna, S. Dasari, S. Karamcheti, S. Nasiriany, M. K. Srirama, L. Y. Chen, K. Ellis, et al. Droid: A large-scale in-the-wild robot manipulation dataset. *arXiv preprint arXiv:2403.12945*, 2024.
- [5] S. Nair, A. Rajeswaran, V. Kumar, C. Finn, and A. Gupta. R3m: A universal visual representation for robot manipulation. *arXiv preprint arXiv:2203.12601*, 2022.
- [6] A. Majumdar, K. Yadav, S. Arnaud, Y. J. Ma, C. Chen, S. Silwal, A. Jain, V.-P. Berges, P. Abbeel, J. Malik, et al. Where are we in the search for an artificial visual cortex for embodied intelligence? *arXiv preprint arXiv:2303.18240*, 2023.
- [7] T. Xiao, I. Radosavovic, T. Darrell, and J. Malik. Masked visual pre-training for motor control. *arXiv preprint arXiv:2203.06173*, 2022.
- [8] S. Parisi, A. Rajeswaran, S. Purushwalkam, and A. Gupta. The unsurprising effectiveness of pre-trained vision models for control. *arXiv preprint arXiv:2203.03580*, 2022.
- [9] S. Karamcheti, S. Nair, A. S. Chen, T. Kollar, C. Finn, D. Sadigh, and P. Liang. Language-driven representation learning for robotics. *arXiv preprint arXiv:2302.12766*, 2023.
- [10] B. Zitkovich, T. Yu, S. Xu, P. Xu, T. Xiao, F. Xia, J. Wu, P. Wohlhart, S. Welker, A. Wahid, et al. Rt-2: Vision-language-action models transfer web knowledge to robotic control. In *Conference on Robot Learning*, pages 2165–2183. PMLR, 2023.
- [11] N. D. Palo and E. Johns. Dinobot: Robot manipulation via retrieval and alignment with vision foundation models. In *IEEE International Conference on Robotics and Automation (ICRA)*, 2024.
- [12] M. J. Kim, K. Pertsch, S. Karamcheti, T. Xiao, A. Balakrishna, S. Nair, R. Rafailov, E. Foster, G. Lam, P. Sanketi, et al. Openvla: An open-source vision-language-action model. *arXiv preprint arXiv:2406.09246*, 2024.
- [13] K. Black, M. Nakamoto, P. Atreya, H. Walke, C. Finn, A. Kumar, and S. Levine. Zero-shot robotic manipulation with pretrained image-editing diffusion models. *arXiv preprint arXiv:2310.10639*, 2023.
- [14] H. Bharadhwaj, A. Gupta, and S. Tulsiani. Visual affordance prediction for guiding robot exploration. In *2023 IEEE International Conference on Robotics and Automation (ICRA)*, pages 3029–3036. IEEE, 2023.
- [15] I. Kapelyukh, V. Vosylius, and E. Johns. Dall-e-bot: Introducing web-scale diffusion models to robotics. *IEEE Robotics and Automation Letters*, 8(7):3956–3963, 2023.
- [16] H. Bharadhwaj, A. Gupta, V. Kumar, and S. Tulsiani. Towards generalizable zero-shot manipulation via translating human interaction plans. In *2024 IEEE International Conference on Robotics and Automation (ICRA)*, 2024.

- 347 [17] H. Bharadhwaj, R. Mottaghi, A. Gupta, and S. Tulsiani. Track2act: Predicting point
348 tracks from internet videos enables diverse zero-shot robot manipulation. *arXiv preprint*
349 *arXiv:2405.01527*, 2024.
- 350 [18] R. Girdhar, M. Singh, A. Brown, Q. Duval, S. Azadi, S. S. Rambhatla, A. Shah, X. Yin,
351 D. Parikh, and I. Misra. Emu video: Factorizing text-to-video generation by explicit image
352 conditioning. *arXiv preprint arXiv:2311.10709*, 2023.
- 353 [19] C. Saharia, W. Chan, S. Saxena, L. Li, J. Whang, E. Denton, S. K. S. Ghasemipour, B. K.
354 Ayan, S. S. Mahdavi, R. G. Lopes, et al. Photorealistic text-to-image diffusion models with
355 deep language understanding. *arXiv preprint arXiv:2205.11487*, 2022.
- 356 [20] D. Kondratyuk, L. Yu, X. Gu, J. Lezama, J. Huang, R. Hornung, H. Adam, H. Akbari, Y. Alon,
357 V. Birodkar, et al. Videopoet: A large language model for zero-shot video generation. *arXiv*
358 *preprint arXiv:2312.14125*, 2023.
- 359 [21] C. Doersch, Y. Yang, D. Gokay, P. Luc, S. Koppula, A. Gupta, J. Heyward, R. Goroshin,
360 J. Carreira, and A. Zisserman. Bootstap: Bootstrapped training for tracking-any-point. *arXiv*
361 *preprint arXiv:2402.00847*, 2024.
- 362 [22] C. Finn, T. Yu, T. Zhang, P. Abbeel, and S. Levine. One-shot visual imitation learning via
363 meta-learning. In *Conference on robot learning*, pages 357–368. PMLR, 2017.
- 364 [23] S. Young, D. Gandhi, S. Tulsiani, A. Gupta, P. Abbeel, and L. Pinto. Visual imitation made
365 easy. In *Conference on Robot Learning (CoRL)*, 2020.
- 366 [24] A. Mandlekar, Y. Zhu, A. Garg, J. Booher, M. Spero, A. Tung, J. Gao, J. Emmons, A. Gupta,
367 E. Orbay, et al. Roboturk: A crowdsourcing platform for robotic skill learning through imita-
368 tion. In *Conference on Robot Learning*, pages 879–893. PMLR, 2018.
- 369 [25] S. Ross, N. Melik-Barkhudarov, K. S. Shankar, A. Wendel, D. Dey, J. A. Bagnell, and
370 M. Hebert. Learning monocular reactive uav control in cluttered natural environments. In
371 *2013 IEEE international conference on robotics and automation*, pages 1765–1772. IEEE,
372 2013.
- 373 [26] Z. Chen and X. Huang. End-to-end learning for lane keeping of self-driving cars. In *2017*
374 *IEEE intelligent vehicles symposium (IV)*, pages 1856–1860. IEEE, 2017.
- 375 [27] A. Mandlekar, Y. Zhu, A. Garg, J. Booher, M. Spero, A. Tung, J. Gao, J. Emmons, A. Gupta,
376 E. Orbay, et al. Roboturk: A crowdsourcing platform for robotic skill learning through imita-
377 tion. In *Conference on Robot Learning*, pages 879–893. PMLR, 2018.
- 378 [28] E. Jang, A. Irpan, M. Khansari, D. Kappler, F. Ebert, C. Lynch, S. Levine, and C. Finn. Bc-z:
379 Zero-shot task generalization with robotic imitation learning. In *Conference on Robot Learn-*
380 *ing*, pages 991–1002. PMLR, 2022.
- 381 [29] H. R. Walke, K. Black, T. Z. Zhao, Q. Vuong, C. Zheng, P. Hansen-Estruch, A. W. He, V. My-
382 ers, M. J. Kim, M. Du, et al. Bridgedata v2: A dataset for robot learning at scale. In *Conference*
383 *on Robot Learning*, pages 1723–1736. PMLR, 2023.
- 384 [30] D. Kalashnikov, A. Irpan, P. Pastor, J. Ibarz, A. Herzog, E. Jang, D. Quillen, E. Holly,
385 M. Kalakrishnan, V. Vanhoucke, et al. Scalable deep reinforcement learning for vision-based
386 robotic manipulation. In *Conference on robot learning*, pages 651–673. PMLR, 2018.
- 387 [31] K. Grauman, A. Westbury, E. Byrne, Z. Chavis, A. Furnari, R. Girdhar, J. Hamburger, H. Jiang,
388 M. Liu, X. Liu, et al. Ego4d: Around the world in 3,000 hours of egocentric video. In
389 *Proceedings of the IEEE/CVF Conference on Computer Vision and Pattern Recognition*, pages
390 18995–19012, 2022.

- 391 [32] J. Deng, W. Dong, R. Socher, L.-J. Li, K. Li, and L. Fei-Fei. Imagenet: A large-scale hierar-
392 chical image database. In *2009 IEEE conference on computer vision and pattern recognition*,
393 pages 248–255. Ieee, 2009.
- 394 [33] Y. J. Ma, S. Sodhani, D. Jayaraman, O. Bastani, V. Kumar, and A. Zhang. Vip: Towards
395 universal visual reward and representation via value-implicit pre-training. *arXiv preprint*
396 *arXiv:2210.00030*, 2022.
- 397 [34] S. Parisi, A. Rajeswaran, S. Purushwalkam, and A. Gupta. The unsurprising effectiveness of
398 pre-trained vision models for control. *arXiv preprint arXiv:2203.03580*, 2022.
- 399 [35] H. Wu, Y. Jing, C. Cheang, G. Chen, J. Xu, X. Li, M. Liu, H. Li, and T. Kong. Unleash-
400 ing large-scale video generative pre-training for visual robot manipulation. *arXiv preprint*
401 *arXiv:2312.13139*, 2023.
- 402 [36] S. Yang, J. Walker, J. Parker-Holder, Y. Du, J. Bruce, A. Barreto, P. Abbeel, and D. Schu-
403 urmans. Video as the new language for real-world decision making. *arXiv preprint*
404 *arXiv:2402.17139*, 2024.
- 405 [37] M. Sharma, C. Fantacci, Y. Zhou, S. Koppula, N. Heess, J. Scholz, and Y. Aytar. Lossless adap-
406 tation of pretrained vision models for robotic manipulation. *arXiv preprint arXiv:2304.06600*,
407 2023.
- 408 [38] N. Hansen, Z. Yuan, Y. Ze, T. Mu, A. Rajeswaran, H. Su, H. Xu, and X. Wang. On pre-
409 training for visuo-motor control: Revisiting a learning-from-scratch baseline. *arXiv preprint*
410 *arXiv:2212.05749*, 2022.
- 411 [39] Z. Mandi, H. Bharadhwaj, V. Moens, S. Song, A. Rajeswaran, and V. Kumar. Cacti:
412 A framework for scalable multi-task multi-scene visual imitation learning. *arXiv preprint*
413 *arXiv:2212.05711*, 2022.
- 414 [40] Z. Chen, S. Kiami, A. Gupta, and V. Kumar. Genau: Retargeting behaviors to unseen situa-
415 tions via generative augmentation. *arXiv preprint arXiv:2302.06671*, 2023.
- 416 [41] T. Yu, T. Xiao, A. Stone, J. Tompson, A. Brohan, S. Wang, J. Singh, C. Tan, J. Peralta,
417 B. Ichter, et al. Scaling robot learning with semantically imagined experience. *arXiv preprint*
418 *arXiv:2302.11550*, 2023.
- 419 [42] Z. Chen, Z. Mandi, H. Bharadhwaj, M. Sharma, S. Song, A. Gupta, and V. Kumar. Se-
420 mantically controllable augmentations for generalizable robot learning. *arXiv preprint*
421 *arXiv:2409.00951*, 2024.
- 422 [43] C. Wang, L. Fan, J. Sun, R. Zhang, L. Fei-Fei, D. Xu, Y. Zhu, and A. Anandkumar. Mimicplay:
423 Long-horizon imitation learning by watching human play. *arXiv preprint arXiv:2302.12422*,
424 2023.
- 425 [44] L. Smith, N. Dhawan, M. Zhang, P. Abbeel, and S. Levine. Avid: Learning multi-stage tasks
426 via pixel-level translation of human videos. *arXiv*, 2019.
- 427 [45] H. Xiong, Q. Li, Y.-C. Chen, H. Bharadhwaj, S. Sinha, and A. Garg. Learning by watching:
428 Physical imitation of manipulation skills from human videos. *arXiv*, 2021.
- 429 [46] V. Jain, M. Attarian, N. J. Joshi, A. Wahid, D. Driess, Q. Vuong, P. R. Sanketi, P. Sermanet,
430 S. Welker, C. Chan, et al. Vid2robot: End-to-end video-conditioned policy learning with cross-
431 attention transformers. *arXiv preprint arXiv:2403.12943*, 2024.
- 432 [47] C. Wen, X. Lin, J. So, K. Chen, Q. Dou, Y. Gao, and P. Abbeel. Any-point trajectory modeling
433 for policy learning. *arXiv preprint arXiv:2401.00025*, 2023.

- 434 [48] J. Gu, S. Kirmani, P. Wohlhart, Y. Lu, M. G. Arenas, K. Rao, W. Yu, C. Fu, K. Gopalakrishnan,
435 Z. Xu, et al. Rt-trajectory: Robotic task generalization via hindsight trajectory sketches. *arXiv*
436 *preprint arXiv:2311.01977*, 2023.
- 437 [49] Y. Qin, Y.-H. Wu, S. Liu, H. Jiang, R. Yang, Y. Fu, and X. Wang. Dexmv: Imitation learning
438 for dexterous manipulation from human videos. *arXiv preprint arXiv:2108.05877*, 2021.
- 439 [50] K. Shaw, S. Bahl, and D. Pathak. Videodex: Learning dexterity from internet videos. In *6th*
440 *Annual Conference on Robot Learning*.
- 441 [51] K. Mo, L. J. Guibas, M. Mukadam, A. Gupta, and S. Tulsiani. Where2act: From pixels to
442 actions for articulated 3d objects. In *Proceedings of the IEEE/CVF International Conference*
443 *on Computer Vision*, pages 6813–6823, 2021.
- 444 [52] M. Goyal, S. Modi, R. Goyal, and S. Gupta. Human hands as probes for interactive object
445 understanding. In *Proceedings of the IEEE/CVF Conference on Computer Vision and Pattern*
446 *Recognition*, pages 3293–3303, 2022.
- 447 [53] S. Bahl, R. Mendonca, L. Chen, U. Jain, and D. Pathak. Affordances from human videos as a
448 versatile representation for robotics. In *CVPR*, 2023.
- 449 [54] S. Liu, S. Tripathi, S. Majumdar, and X. Wang. Joint hand motion and interaction hotspots
450 prediction from egocentric videos. In *Proceedings of the IEEE/CVF Conference on Computer*
451 *Vision and Pattern Recognition*, pages 3282–3292, 2022.
- 452 [55] C. Yuan, C. Wen, T. Zhang, and Y. Gao. General flow as foundation affordance for scalable
453 robot learning. *arXiv preprint arXiv:2401.11439*, 2024.
- 454 [56] S. Bahl, A. Gupta, and D. Pathak. Human-to-robot imitation in the wild. *RSS*, 2022.
- 455 [57] Y. Du, S. Yang, B. Dai, H. Dai, O. Nachum, J. Tenenbaum, D. Schuurmans, and P. Abbeel.
456 Learning universal policies via text-guided video generation. *Advances in Neural Information*
457 *Processing Systems*, 36, 2024.
- 458 [58] J. Liang, R. Liu, E. Ozguroglu, S. Sudhakar, A. Dave, P. Tokmakov, S. Song, and C. Von-
459 drick. Dreamitate: Real-world visuomotor policy learning via video generation. *arXiv preprint*
460 *arXiv:2406.16862*, 2024.
- 461 [59] G. Papagiannis, N. Di Palo, P. Vitiello, and E. Johns. R+ x: Retrieval and execution from
462 everyday human videos. *arXiv preprint arXiv:2407.12957*, 2024.
- 463 [60] J.-B. Alayrac, J. Donahue, P. Luc, A. Miech, I. Barr, Y. Hasson, K. Lenc, A. Mensch, K. Mil-
464 lican, M. Reynolds, et al. Flamingo: a visual language model for few-shot learning. *Advances*
465 *in neural information processing systems*, 35:23716–23736, 2022.
- 466 [61] C. Doersch, A. Gupta, L. Markeeva, A. Recasens, L. Smaira, Y. Aytar, J. Carreira, A. Zis-
467 serman, and Y. Yang. Tap-vid: A benchmark for tracking any point in a video. *Advances in*
468 *Neural Information Processing Systems*, 35:13610–13626, 2022.
- 469 [62] G. Team, R. Anil, S. Borgeaud, Y. Wu, J.-B. Alayrac, J. Yu, R. Soricut, J. Schalkwyk, A. M.
470 Dai, A. Hauth, et al. Gemini: a family of highly capable multimodal models. *arXiv preprint*
471 *arXiv:2312.11805*, 2023.
- 472 [63] N. Karaev, I. Rocco, B. Graham, N. Neverova, A. Vedaldi, and C. Rupprecht. Cotracker: It is
473 better to track together. *arXiv preprint arXiv:2307.07635*, 2023.
- 474 [64] G. Le Moing, J. Ponce, and C. Schmid. Dense optical tracking: connecting the dots. In
475 *Proceedings of the IEEE/CVF Conference on Computer Vision and Pattern Recognition*, pages
476 19187–19197, 2024.

477 Appendix

478 Here we provide additional details on the method and experiments of *Gen2Act*.

479 5.1 Human Video Generation

480 We use a pre-trained VideoPoet model [20] directly without any adaptation or fine-tuning. The input
481 to the model for video generation is a language description of a task (the prompt) and a square-
482 shaped image. By virtue of being trained on diverse large-scale video datasets ($> 270M$ videos)
483 we find that this model generalizes well to everyday tasks we develop *Gen2Act* for. It can gener-
484 ate realistic and plausible videos of humans manipulating objects, without introducing significant
485 camera motions/artifacts in the generated videos. We ensure that the image of the scene input to
486 the model doesn't have the robot in the frame (the initial reset position of the robot is such that
487 the arm is mostly out of camera view). The language prompt to the model is of the form "A per-
488 son `task-name`, static camera" e.g. for the task 'opening the microwave' the input prompt is "A
489 person opening the microwave, static camera."

490 5.2 Closed-Loop Policy

491 For each frame in the generated human video \mathbf{V}_g and the robot video $\mathbf{I}_{t-k:k}$, we first extract features,
492 i_g and i_r through a ViT encoder χ . The number of video tokens extracted this way is very large
493 and they are temporally uncorrelated, so we have Transformer encoders Φ_g and Φ_r that process
494 the respective video tokens through gated Cross-Attention Layers based on a Perceiver-Resampler
495 architecture [60] and output a fixed number $N = 64$ of tokens. We use 2 Perceiver-Resampler layers
496 for both the generated video token processing and the robot observation history video processing.
497 These tokens respectively are $z_g = \Phi_g(i_g)$ and $z_r = \Phi_r(i_r)$. During training we sample a fixed
498 sequence of 16 frames from the generated video ensuring that we always sample the first and last
499 frames. For the robot history, we choose the last 8 frames of robot observations. We resize all
500 images to 224x224 dimensions.

501 We run an off-the-shelf tracking model [61, 21] on the generated video \mathbf{V}_g to obtain tracks τ_g of
502 a random set of points in the first frame P^0 . In order to ensure that the latent embeddings from
503 the generated video z_g can distill motion information in the video, we set up a track prediction task
504 conditioned on the video tokens. For this, we define a track prediction transformer $\psi_g(P^0, i_g^0, z_g)$
505 to predict tracks $\hat{\tau}_g$ and define an auxiliary loss $\|\tau_g - \hat{\tau}_g\|_2$ to update tokens g_e . Similarly, for the
506 current robot video $\mathbf{I}_{t-k:k}$, we set up a similar track prediction auxiliary loss. We run the ground-
507 truth track prediction once over the entire robot observation sequence (again with random points in
508 the first frame P_0), but during training, the policy is input a chunk of length k in one pass. So here,
509 the track prediction transformer $\psi_r(P^{t-k}, i_{t-k}, r_e^{t-k:t})$ is conditioned on the points in the beginning
510 of the chunk P_{t-k} , the image features at that time-step i^{t-k} and the observation tokens for the chunk
511 z_r . The track prediction transformer has 6 self-attention layers with 8 heads and its role is solely
512 to make the input tokens from generated video / robot observations informative of motion cues.
513 Note that any ground-truth track prediction model can be used for this, and recent advances in point
514 tracking can help improve this step [63, 64]

515 For ease of prediction, we discretize the action space such that each dimension has 256 bins. So
516 each action dimension can take values in the range $[0, 255]$. The bins are uniformly distributed
517 within the bounds of each dimension. We predict actions in the end-effector space, and also predict
518 whether to terminate the episode, and whether the gripepr should be open/close. We optimize a
519 Behavior Cloning (BC) objective by minimizing error between the predicted actions $\hat{a}_{t:t+h}$ and the
520 ground-truth $a_{t:t+h}$ through a cross-entropy loss. This discrete action-space for prediction is based
521 on prior works in multi-task imitation learning [1].

Table 3: Comparison of success rates for long-horizon activities via chaining of different tasks. We first obtain sub-tasks for activities with an off-the-shelf LLM and then rollout *Gen2Act* in sequence for the different intermediate tasks.

Activity	Stages (from Gemini)	Success % Stage 1, Stage 2, Stage 3
Stowing Apple	<ol style="list-style-type: none"> 1. Open the Drawer 2. Place Apple in Drawer 3. Close the Drawer 	80, 60, 60
Making Coffee	<ol style="list-style-type: none"> 1. Open the Lid 2. Place K-Cup Pod inside 3. Close the Lid 	40, 20, 20
Cleaning Table	<ol style="list-style-type: none"> 1. Pick Tissues from Box 2. Press the Sanitizer Dispenser 3. Wipe the Table with Tissues 	60, 40, 40
Heating Soup	<ol style="list-style-type: none"> 1. Open the Microwave 2. Put Bowl inside Microwave 3. Close the Microwave 	40, 20, 20

522 **5.3 Chaining Gen2Act for Long-Horizon Manipulation**

523 For deploying *Gen2Act* to solve a manipulation task, we first generate a human video conditioned on
524 the language description of the task and the image of the scene. We then roll out the generated video
525 conditioned closed-loop policy. For chaining *Gen2Act* to perform long-horizon activities consisting
526 of several tasks, we first use an off-the-shelf LLM (e.g. Gemini) to obtain language descriptions of
527 the different tasks. We chain *Gen2Act* for the task sequence by using the last image of the previous
528 policy rollout as the first frame for generating a human video of the subsequent task. We do this
529 chaining in sequence as opposed to generating all the videos from the first image because the final
530 state of the objects in the scene might be different after the robot execution of an intermediate task.
531 This iterative sequencing of video generation after the previous robot execution is made possible by
532 the fast generation capabilities of the Video model we use, VideoPoet (it takes less than 10 seconds
533 to generate a new video after generating the very first video).

534 We provide examples of the prompt to Gemini and the subsequent outputs for task decomposition
535 below:

536 *Cleaning the Table.* Q. What are the steps involved in cleaning a table with sanitizer dispenser and
537 tissues? (write three steps)

538 A: Steps for Cleaning a Table with Sanitizer Dispenser and Tissues:

- 539 • Gather materials: Pick tissues from the box.
- 540 • Apply sanitizer: Press the sanitizer dispenser onto the tissue.
- 541 • Wipe: Gently wipe the table surface with the sanitizer-dampened tissues.

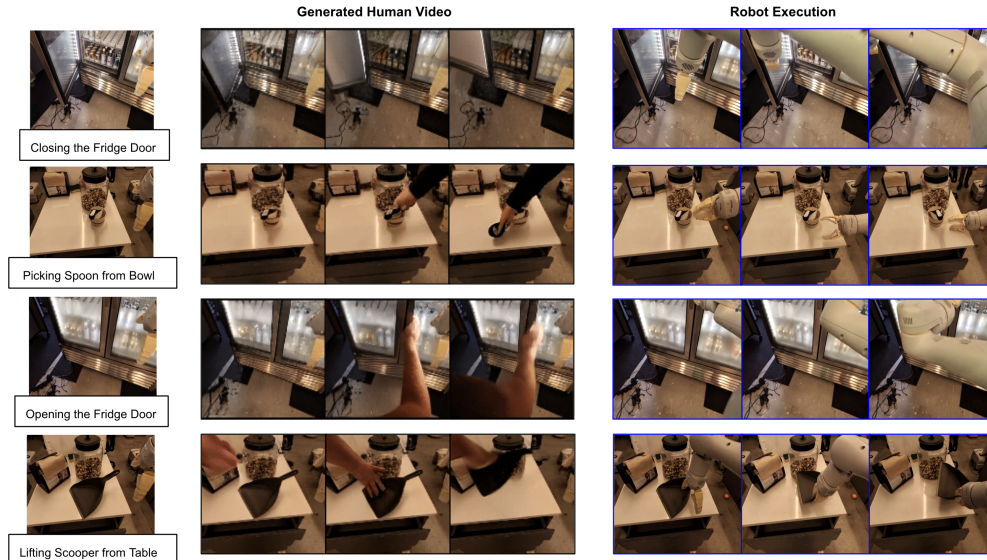


Figure 6: Analysis of failures of *Gen2Act*. The tasks here correspond to object type generalization. We can see that most of the failures of robot execution (top 3 rows) are correlated with incorrect video generations. In the last row the video generation is plausible but the execution is incorrect in following the trajectory of the generated video after grasping the object.

542 *Making Coffee*. Q. What are the steps involved in making coffee with a Keurig? (write first three
543 steps)

544 A: Steps for Making Coffee with a Keurig:

- 545 • Open the lid: Open the lid of the Keurig machine.
- 546 • Insert K-Cup: Place a K-Cup pod into the machine.
- 547 • Close the lid: Close the lid of the Keurig machine.

548 Videos for these tasks are best viewed in the project website.

549 **5.4 Analysis of Failures**

550 Here we discuss the type of failures exhibited by *Gen2Act*. We observe that for MG and to some
551 extent in G, inaccuracies in video generation are less correlated with failures of the policy. While, for
552 the higher levels of generalization, object type (OTG) and motion type (MTG), if video generation
553 yields implausible videos, then the policy doesn't succeed in performing the tasks. This is also
554 evidence that the policy of *Gen2Act* is using the generated human video for inferring motion cues
555 while completing a task, and as such when video generation is incorrect in scenarios where robot
556 data support is limited (e.g. in OTG and MTG), the policy fails. Fig. 6 shows some examples of
557 failures of *Gen2Act* in different tasks. Most of the failures are correlated with video generation (first
558 three rows) but generating a video plausibly (fourth row) is not a guarantee of the policy succeeding
559 because there might be issues with grasping the object correctly and following the trajectory of the
560 object post grasp. This indicates potential for future work to explore recovering more dense motion
561 information from the generated videos beyond point tracks, like object meshes for mitigating some
562 of the failures.